Probing the Helical Stability in a VEGF-mimetic Peptide

Lucia De Rosa[1], Donatella Diana[1], Rossella Di Stasi[1], Alessandra Romanelli[2], Michele F. M. Sciacca[3], Danilo Milardi[3], Carla Isernia[4], Roberto Fattorusso[4], Luca D. D'Andrea[5*]

[1]Istituto di Biostrutture e Bioimmagini, Consiglio Nazionale delle Ricerche, Napoli, Italy

[2]Dipartimento di Scienze Farmaceutiche, Università degli Studi di Milano, Milano, Italy

[3]Istituto di Cristallografia, Consiglio Nazionale delle Ricerche, Catania, Italy

[4]Dipartimento di Scienze e Tecnologie Ambientali, Biologiche e Farmaceutiche, Università della Campania "L. Vanvitelli", Caserta, Italy

[5]Istituto di Scienze e Tecnologie Chimiche "Giulio Natta", Consiglio Nazionale delle Ricerche, Milano, Italy

* Corresponding author: Istituto di Scienze e Tecnologie Chimiche "Giulio Natta", CNR, Via Mario Bianco 9, 20131, Milano, Italy; email: luca.dandrea@cnr.it

Keywords: helical, peptide, NMR spectroscopy, DSC, Circular dichroism

Abstract

The analysis of the forces governing helix formation and stability in peptides and proteins has attracted considerable interest in order to shed light on folding mechanism. We analyzed the role of hydrophobic interaction, steric hindrance and chain length on *i, i+3* position in QK peptide, a VEGF mimetic helical peptide. We focused on position 10 of QK, occupied by a leucine, as previous studies highlighted the key role of the Leu7-Leu10 interaction in modulating the helix formation and inducing an unusual thermodynamic stability. Leu10 has been replaced by hydrophobic amino acids with different side-chain length, hydrophobicity and steric hindrance. Ten peptides were, hence, synthesized and analyzed combining circular dichroism, calorimetry and NMR spectroscopy. We found that helical content and thermal stability of peptide QK changed when Leu10 was replaced. Interestingly, we observed that the changes in the helical content and thermal stability were not always correlated and they depend on the type of interaction (strength and geometry) that could be established between Leu7 and the residue in position 10.

1. Introduction

The analysis of molecular forces governing peptide structure formation and stability is crucial to understand the protein folding, to predict protein structure starting from amino acid sequence and to design biomolecules with specific structures and functions. In this context, peptides emerged as appropriate and convenient model systems for understanding the basic principles of protein folding and energetics. In particular, the formation and stability of helical and β-sheet structures were deeply investigated using peptides [1-3] as these secondary structure elements act as nucleation folding units in proteins. Moreover, the design of molecules assuming these pre-organized structures is a useful strategy to modulate protein-protein interactions, with particular interest in drug discovery.

QK is a helical peptide, designed on the VEGF 17-25 helix region, presenting a well characterized biological profile [4] and widely employed to decorate biomaterials for biomedical applications.[5-7] The peptide QK consists of 15 natural amino acids, it exerts its activity through the binding to VEGF receptors on the surface of endothelial cells, and it is capable of inducing a biological response similar to that of VEGF both *in vitro* [4, 8] and *in vivo* [9-12]. QK peptide assumes a stable helical conformation in aqueous solution which is a prerequisite for its biological activity.[4, 13] QK shows an unusual thermal stability whose molecular determinants were analyzed.[14] In particular, we found that the N-terminal region [13] and a hydrophobic interaction (*i, i+3*) involving Leu7 and Leu10 [15] play a relevant role in determining QK helical and thermal stability. In fact, the substitution of Leu10 of QK with Ala (QK10A), a helix stabilizing residue, implicates a decrease of the peptide folded helical population and the loss of the unusual thermal stability.[15] Analysis of the folding pathway of QK10A revealed that the central helical turn (residues from 6 to 9) plays an important role for peptide folding acting as site of helix nucleation. Furthermore, the improved stabilization by hydrophobic effect operated by Leu10 could be considered at the basis of the unusual thermal stability and high helical population of peptide QK.[15]

In this work, designing a series of QK10 mutants, we investigated the role of interacting residues located in QK position 7 and 10 (*i, i+3 spacing)*, evaluating how peptide helical population and thermal stability are affected modifying the properties of the residue in position 10.

2. Experimental section

2.1 Materials

N-9-Fluorenylmethyloxycarbonyl (Fmoc)-protected amino acids, coupling reagents for peptide synthesis and Rink amide resin were provided by Merck-Novabiochem. N,N-diisopropylethylamine (DIPEA) was provided from Romil, while piperidine was purchased from Biosolve. Acetic anhydride and the other solvents for peptide synthesis and purification (dimethylformamide, dichloromethane, trifluoroacetic acid, triisopropylsilane, diethyl ether, acetonitrile) were from Sigma-Aldrich. Mass analysis of peptides was performed on an LC-MS system Agilent 1200 Infinity Series (Agilent Technologies) equipped with a diode array and an ESI-ToF ion source-analyzer using a Jupiter C18 column 150 x 2.0 mm, 300 Å, 3 µ (Phenomenex). Purifications by RP-preparative HPLC were performed on an HP 1200 Series (Agilent Technologies), equipped with a SPD-M10 AV detector, using a Axia 50 x 21.2 mm, Synergi, 4 µ, Fusion RP 80 Å (Phenomenex) or a Jupiter Proteo 250 x 21.2 mm, 90 Å, 10 µ (Phenomenex) at a flow rate of 20 mL/min. Analytical characterization of peptides was performed on an HP 1200 Series (Agilent Technologies), using a Jupiter Proteo C12 column 4.6 x 250 mm, 90 Å, 4 µ (Phenomenex) at a flow rate of 1.0 mL min^{-1}. Circular Dichroism (CD) analyses were performed on a J-810 spectropolarimeter (Jasco, Easton, US) equipped with a PTC-423S/15 Peltier temperature control system, using a 0.1 cm quartz cells (Hellma).

2.2 Synthesis and Purification of Peptides.

Peptides were synthesized on solid phase using Fmoc-protected amino acids on a Rink Amide MBHA (0.51 mmol/g). Coupling of amino acids was performed with an excess of Fmoc-amino acid (10 eq.), 9.9 equivalents of 2-(1H-Benzotriazole-1-yl)-1,1,3,3-tetramethyluronium hexafluorophosphate (HBTU)/N-hydroxybenzotriazole (HOBT) in the presence of 20 equivalents of diisopropylethyl amine (DIPEA) in dimethylformamide (DMF) (1 h, each). α-amine group deprotection was carried

out in 30% piperidine in DMF (2 x 5'). After each amino acid coupling, unreacted α-amine groups were acetylated with a solution of 2 M acetic anhydride, 0.06 M HOBt, 0.55 M DIPEA in NMP (5 min). After each reaction step, 5 washes of 1 min each in DMF were performed to remove exceeding reagents and reaction side products. Once the peptide synthesis was completed, the N-terminal Fmoc group was removed and α-amino group was acetylated. Finally, the resin was treated with DMF (5 x 1'), DCM (5 x 1') and ethyl ether (3 x 1'), and dried under vacuum. Peptide cleavage from the resin and amino acids side-chain deprotection were performed in 95:2.5:2.5 trifluoroacetic acid (TFA): triisopropylsilane (TIS): water at room temperature for 3 h. Crude peptide products were precipitated in cold diethyl-ether, collected by centrifugation, dissolved in a water/acetonitrile mixture and lyophilized. The peptides were purified by RP-preparative HPLC using an AXIA column Axia 50 x 21.2 mm, Synergi, 4 µ, Fusion RP 80 Å (Phenomenex) applying a linear gradient of CH_3CN (0.1% TFA) in H_2O (0.1% TFA) from 20% to 60% in 20 min (20 mL/min) or using a Jupiter Proteo column 250 x 21.2 mm, 10 µ, 90 Å,; (Phenomenex) and a linear gradient of CH_3CN (0.1% TFA) in H_2O (0.1% TFA) from 20% to 70% in 50 minutes (20 mL/min). The peptides purity was assessed by analytical RP-HPLC using a Jupiter Proteo C12 column 4.6 x 150 mm, 90 Å, 4 µ (Phenomenex) at a flow rate of 1.0 mL min^{-1}. A gradient of CH_3CN (0.1% TFA) in H_2O (0.1% TFA) from 20% to 60% in 20 min was used to elute peptides. The identity of the peptides was determined by LC-MS spectrometry on an Agilent 1200 Infinity Series (Agilent Technologies) equipped with a diode array and an ESI-ToF ion source-analyzer, using a Jupiter C18 column 150 x 2.0 mm, 300 Å, 3 µ (Phenomenex) and a gradient of CH_3CN (0.1% TFA) in H_2O (0.1% TFA) from 5% to 70% in 20 min.

2.3 Circular Dichroism spectroscopy

Far UV circular dichroism spectra were recorded on a J-715 spectropolarimeter (Jasco) equipped with a PTC-423S/15 Peltier temperature control system, using a 0.1 cm quartz cells (Hellma). Peptides were dissolved in phosphate buffer (10 mM) pH 7.0. The spectra were acquired at 20°C using a data pitch of 0.2 nm with a scan speed of 10 nm/min, a bandwidth of 2 nm, a response time of 4 seconds. A CD spectrum was the average of three consecutive scans in the range 185-260 nm and each CD

spectrum was corrected for the buffer run under identical conditions. The CD data were expressed as mean residue ellipticity (θ). Spectra processing was obtained by the software Spectra Manager (Jasco). Peptide concentrations were determined by absorbance at 280 nm using a molar extinction coefficient of 8480 $cm^{-1}M^{-1}$.

2.4 Nuclear Magnetic Resonance spectroscopy

All NMR spectra were recorded at 298K on a Varian Inova 600 MHz spectrometer, with a 5-mm inverse-detection cryoprobe equipped with z-gradient, located at IBB-CNR, Napoli. For structure determination of QK10Nle and QK10Tle, 2D DQF-COSY, TOCSY and NOESY spectra of the peptides (1 mM) were recorded in aqueous solution at pH 5.5. TOCSY and NOESY experiments were run with mixing times of 70 and 250 ms, respectively. Each of the 512 spectra contained 2048 data points and 64 scans, and had a sweep width of 7000 Hz in both dimensions. Water suppression was achieved by means of Double Pulsed Field Gradient Spin Echo (DPFGSE) sequence[16, 17]. Double quantum filtered spectroscopy (DQF-COSY)[18] was recorded with 4096 data points in the direct dimension and with 500 increments each comprising 64 scans to obtain enough resolution to measure the $^{3}J_{HNH\alpha}$ coupling constants.

1D 1H spectrum was analyzed by using ChemAxon software (http://www.chemaxon.com) while bi-dimesional spectra were processed with SPARKY[19] and analyzed with CARA (Computer Aided Resonance Assignment) software[20] (http://cara.nmr.ch).

The NOE-based distance restraints were obtained from NOESY spectra. The NOE cross peaks were integrated and converted into upper distance bounds using CALIBA program incorporated into the program package CYANA 2.1.[21] The structure analysis and the color figures have been performed with the program MOLMOL[22] and PyMOL[23] (https://pymol.org/2/).

Thermal unfolding of QK10Nle peptide was studied by 2D-TOCSY acquired spetra at 298, 303, 308, 313, 318, 323, 328, 333, 338 and 343 K. All the spectra were acquired consecutively. NMR experiments were carried out in a Varian Inova 400 MHz spectrometer, where the probe temperature

was regularly calibrated by using methanol and ethylenglycol.[24] Denaturation curves were obtained by fitting with a sigmoidal function using GraphPad Prism5 software.

A single step function:

$$Y = A2+B*x+(A1-A2) / (1+\exp((x-x0)/dx))$$

resulted in stable fits with no systematic deviations from the experimental curve, where A1 and A2 are the starting and the final amplitudes, B is the slope of baseline, x0 is the midpoint or transition point, and dx is the slope at x0.[25]

Helix population was estimated from the deviation of Hα chemical shift values (ΔδHα). ΔδHα values from all the residues were averaged and the resulting mean divided by ΔδHα value corrisponding to 100% helix.[26] Values of H random-coil chemical shifts were taken from Wuthrich.[27]

2.5 Differential Scanning Calorimetry

Heating runs were performed in a VP-DSC calorimeter (MicroCal). All samples were degassed under vacuum and scanned at a heating rate of 1 °C min^{-1} in the temperature range 20–120 °C in neutral pure water. Peptide concentrations was in the range 500-700 μM. An extra external pressure of about 29 psi was applied to the solution to prevent the formation of air bubbles during heating. To ensure a complete equilibration of the calorimeter, several buffer−buffer heating scans were routinely performed before measurements. Only after obtaining invariant buffer−buffer baselines samples were scanned. Additional buffer−buffer baselines were obtained immediately after the protein scans to double-check for uncontrolled drifts in instrumental baseline. For each sample, three independent DSC experiments were carried out under the same buffer conditions. To obtain the heat capacity Cp curves, buffer–buffer base lines were recorded at the same scanning rate and then subtracted from sample curves, as previously described.[28, 29] In all experiments, one or several heating−cooling cycles were carried out to determine the reversibility of the denaturation process. To obtain the excess heat capacity profiles (Cp_{exc}), the DSC curves, after instrumental baseline correction, were subtracted from a baseline obtained by a third-order polynomial fit of the pre- and post- transition Cp trends as reported elsewhere.[30, 31]

3. Results

3.1 Peptide design

We designed QK analogue peptides replacing Leu10 with natural and unnatural amino acids presenting side-chains of different length, hydrophobicity and steric hindrance (Table S1). For example, inserting unnatural amino acids such as 2-aminobutyric acid (Abu), nor-valine (Nva) and nor-leucine (Nle), peptides with a straight carbon side-chain of different length were obtained; the effect of the increase of steric hindrance on the β- or γ-carbon was evaluated introducing, respectively, Ala, Val, ter-butylglycine (Tle), phenylglycine (Phg), Nva or Leu; the effect of the presence of an aromatic group at different distance from the backbone was evaluated replacing Leu10 with phenylglycine (Phg) and Phe. The peptides were synthesized in solid phase by Fmoc/tBu chemistry. The identity and purity of the peptides were assessed by HPLC and mass spectrometry (Figure S1).

3.2 Circular dichroism analysis

The conformational properties of peptides were analyzed using circular dichroism (CD) spectroscopy in phosphate buffer at pH = 7.0. The CD spectrum of a peptide in helical conformation is characterized by ~~a~~ two negative minima around 222 nm and 208 nm, a positive maximum around 190 nm, and a crossover point (λ_0) around 200 nm; contrariwise, a peptide in unordered conformation~~s~~ displays a CD spectrum characterized by a deep minimum around 200 nm.[32]

CD spectra analysis showed that the replacement of leucine residue in position 10 impacts on the helical content of peptides (Fig. 1), as assessed by evaluating the variation of the value of mean residue ellipticity at 222 nm (θ_{222}) (Table S2).

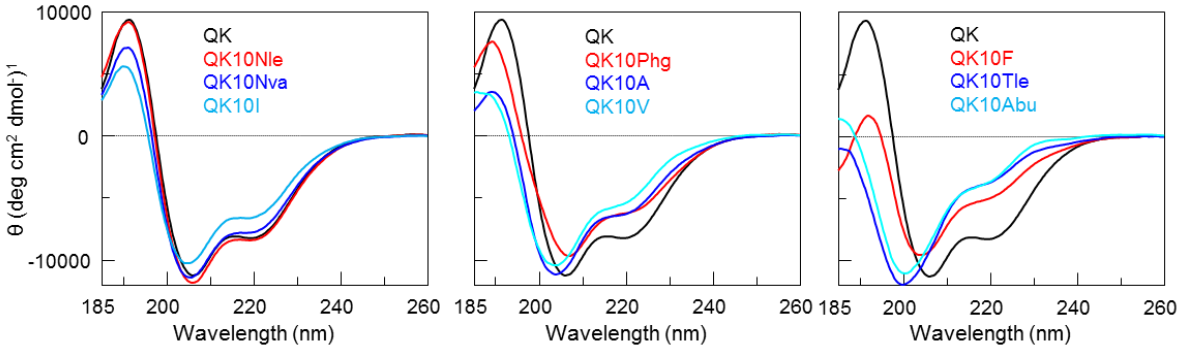

Figure 1: Circular dichroism spectra of QK analogue peptides in 10 mM potassium phosphate buffer at pH 7.0. Spectra are reported as mean residue ellipticity (θ).

QK analogue peptides possess three aromatic residues (one Trp e two Tyr) and, therefore, the absolute helical population could not be precisely estimated because of aromatic residues contribution to θ_{222}.[33] However, θ_{222} can be used to compare the helical content of QK analogue peptides which share the same aromatic residues, except for QK10F and QK10Phg that bear one extra phenyl ring. Typical CD spectra of helical folded peptides were obtained replacing Leu10 with Nle, Ile or Nva, while a modest but significant decrease of peptide helical content is observed introducing Ala, Ile or Phg. In presence of Val or Phe at peptide position 10 the minimum at 222 nm is significantly smoothed, resulting in 40% helical content reduction. Finally, the CD spectra of QK10Tle and QK10Abu peptides showed a minimum around 200 nm and a slight shoulder at 222 nm, suggesting that peptides predominantly assume an unordered conformation with a residual helical population.

3.3 Differential Scanning Calorimetry analysis

Thermal unfolding of QK and its analogues was analyzed by Differential Scanning Calorimetry (DSC). We determined the heat capacity (Cp) in pure water pH 7.0 in the temperature range 20-120 °C with a heating rate of 1 K/min.

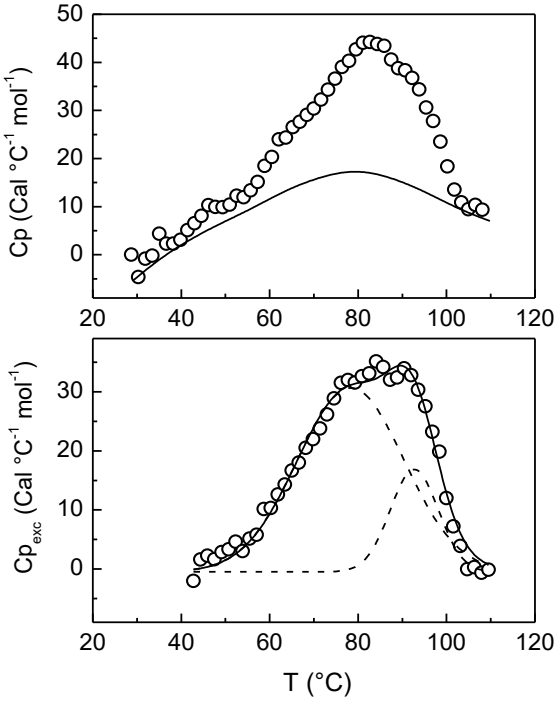

Figure 2: Upper panel. Representative heat capacity (Cp) traces *vs* temperature (open circles) and its relative baseline (solid line) of peptide QK (700 μM) in aqueous solution (pH 7) obtained at a heating rate of 1°C/min. Lower panel. Excess heat capacity (Cp_{exc}) curve (open circles) obtained from Cp values after baseline correction. The experimental data were fitted with a simulated curve (solid line) which is the sum of two gaussian components (dashed lines). The optimized parameters obtained after the non-linear square fitting are reported in table 1.

The DSC profile of QK shows a very broad and weak heat absorption ranging from 55 to 105 °C (Fig. 2). The excess heat capacity function (Cp_{exc}) may be described, at a first approximation, as the sum of two endothermic events centered at 78.3 °C and 92.7 °C. The first of these two unfolding phenomena involves a higher enthalpy change if compared to the second one (Table 1). The second calorimetric peak may be ascribed to the formation at elevated temperature of peptide-peptide interactions, likely favored by the high peptide concentration (700 μM). The occurrence of poorly structured peptide assemblies is also confirmed by the absence of calorimetric reversibility; i.e., a

second DSC run of a previously scanned sample showed only a very small endothermic peak (data not shown). This means that the thermal unfolding of QK cannot be directly analyzed in terms of thermodynamics functions.

Table 1. Fitting parameters of the Cp_{exc} curves relative to the thermal unfolding of QK analogues. The non-linear square fitting was performed with one (QK10A, QKPhg, QK10Abu) or two (QK, QK10I, QK10Nle, QK10V, QK10Nva, QK10F, QK10Tle) gaussian peaks.

Peptide	**1st component**		**2nd component**	
	T_m (°C)	**ΔH (cal mol^{-1})**	**T_m (°C)**	**ΔH (cal mol^{-1})**
QK	78.3 ± 0.1	942 ± 45	92.7 ± 0.1	236 ± 36
QK10Nle	40.7 ± 0.3	430± 21	58.8 ± 0.2	643 ± 32
QK10Nva	50.4 ± 0.3	1441 ± 58	71.4 ± 0.4	1177 ± 59
QK10I	50.6 ± 1.2	2033 ± 168	71.1 ± 0.4	1243 ± 157
QK10Phg	39.1 ± 0.1	1549 ± 50	-	-
QK10A	47.6 ± 0.3	2013 ± 28	-	-
QK10V	41.2 ± 0.2	705 ± 35	57.9 ± 1.0	1416 ± 70
QK10F	39.1 ± 0.3	1219 ± 50	53.8 ± 0.3	769 ± 52
QK10Tle	34.9 ± 0.3	590 ± 122	49.6 ± 2.2	676 ± 148
QK10Abu	41.6 ± 0.2	1074 ± 53	-	-

DSC analysis of QK analogues revealed that the peptides show a melting temperature (T_{M1}) in the range 34.9 – 50.6 °C, indicating a substantial loss of thermodynamic stability when Leu10 is replaced with the reported non-polar amino acids. This thermodynamic destabilization, with respect to peptide QK, is particularly evident for peptide QK10Nle which has a helical content comparable with QK. Peptide QK10Nle shows two endotherms centered at T_{m1} = 40.7 °C and T_{m2} = 58.8 °C, characterized by rather similar enthalpy changes (i.e. ΔH_1 = 430 Cal mol^{-1} and ΔH_2 = 643 Cal mol^{-1} respectively).

The peak centered at 58.8 °C is ascribable, as in QK, to the melting of non-covalent peptide assemblies, likely occurring on unfolded peptide after the first melting. We are inclined to attribute the presence of a second melting curve to this phenomenon also for the peptides QK10I, QK10Nva, QK10V, QK10F, QK10Tle.

3.4 Structural investigation by NMR spectroscopy

Conformational properties of all peptides were firstly explored in H_2O at pH 5.5. The ^{1}H NMR and natural abundance [^{1}H, ^{15}N] HSQC spectra (Fig. S3 and S4) show good chemical shift dispersion, revealing the occurrence of a consistent amount of folded population in all molecules. Almost complete proton resonance assignments were achieved for all peptides (Table S3-S10) by a combination of 2D [^{1}H, ^{1}H] TOCSY, and NOESY 2D data sets (Fig. S5).

The Hα chemical shifts analysis, performed using chemical shift index [34] (Fig. 3a-i), revealed the occurrence of some helical conformation for all peptides; however, QK10Nle, QK10Nva and QK10I peptides strongly tend to form helix, in agreement with the CD data.

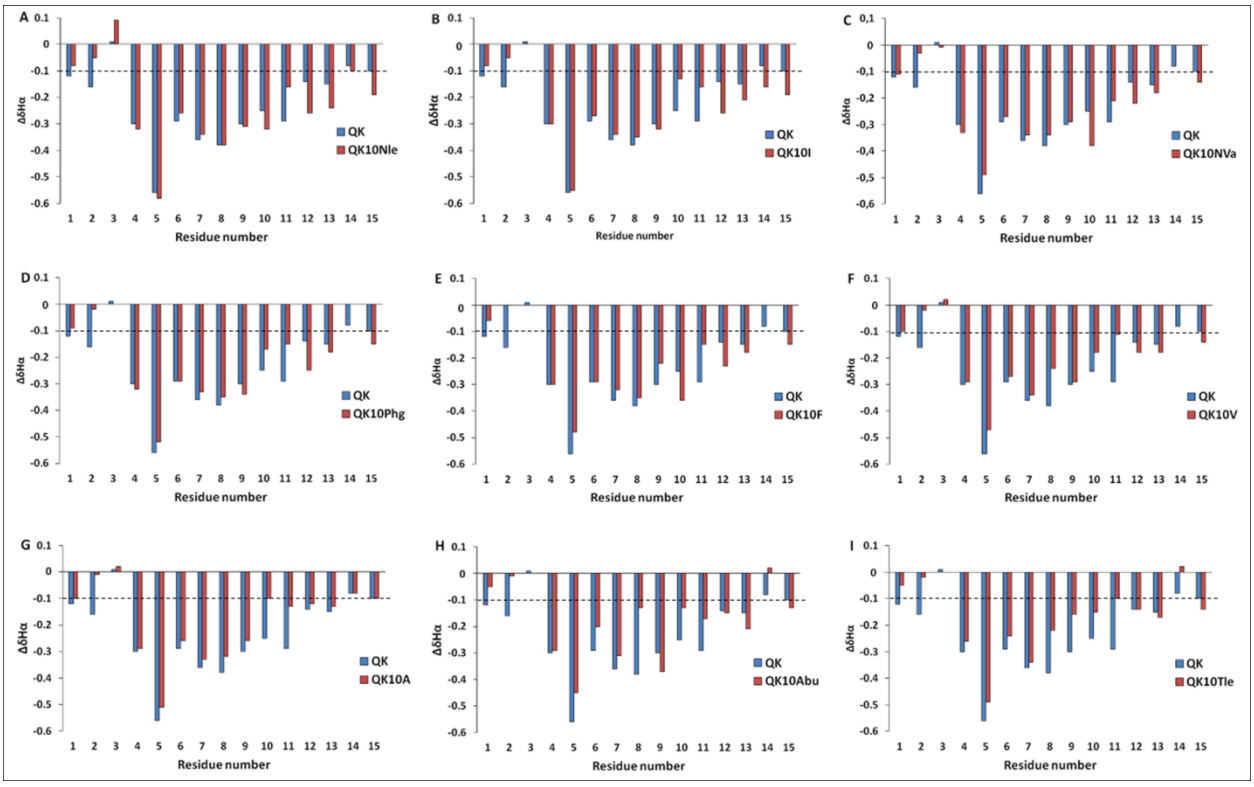

Figure 3: Secondary structure propensity of peptides. The Hα chemical shift analysis was performed by using the random coil values. Dashed lines in the panels indicate the cut-off values for the identification of secondary structure elements as defined by Wishart et al.[34, 35] in the chemical shift index methodology.

The estimated percentage of helical populations (Fig. 4) based on Hα chemical shift of all residues ranges from 59.8% of QK10Nle to 42.0% of QK10Tle.

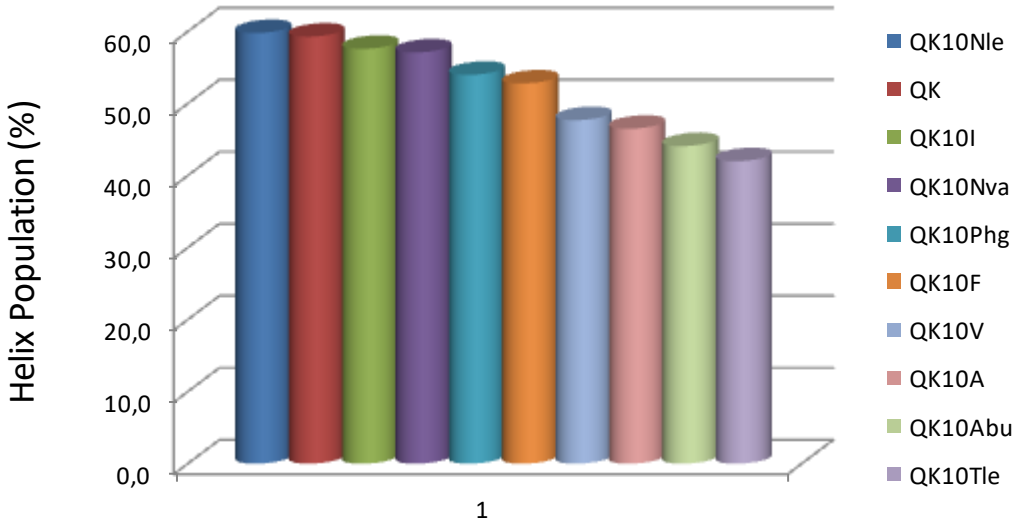

Figure 4: Percentages of helical populations for QK analogue peptides derived from Hα chemical shifts.

Next, the preferred conformations of QK10Nle and QK10Tle, which show the higher and lower helix populations respectively, were calculated by NMR. Identification of spin systems and assignment of individual resonances for QK10Nle and QK10Tle were obtained by a combination of double quantum filtered (DQF)-COSY and TOCSY spectra and a sequence-specific assignment was obtained by NOESY experiment (Fig. S5).

NMR analysis of QK10Nle peptide indicated several NOE contacts characteristic of a helical fold, such HN–HN (i, i+1), Hα– Hα (i, i+3), and Hα–Hβ (i, i+3) net of cross peaks (Fig. S6a) primarily observed in the region encompassing residues W4-K13. The final input (Table S11) for the torsion angle dynamics program (CYANA) for calculation of the structure of QK10Nle consisted of a total of 188 NOE constraints (110 intra-residue, 40 short, and 38 medium range) and 70 torsion angle restraints. The QK10Nle structure (Fig. 5a) consists of a helix spanning the residues from Trp4 to Tyr12 and of two more disordered N- and C-terminal tails. The rms deviation values of the backbone and of all heavy atoms of the 4-12 region of QK10Nle are 0.10±0.03 Å and 0.85±0.20 Å, respectively (Fig. 5a and b). Although being more populated than in the QK peptide, as shown by CD spectra and CSI analyses, the helical conformation in QK10Nle involves the same central region, which is helical in QK. Indeed, superposition of QK10Nle and QK representative structures (Fig. 5c, S7) indicates that the two peptides fold very similarly with a rms deviation 0.68±0.11 Å but nonetheless exhibit structural differences at the C-terminus.

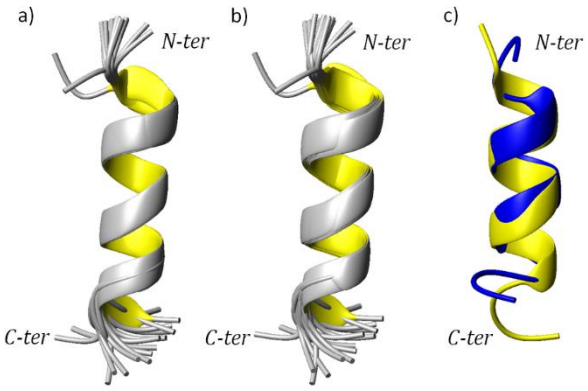

Figure 5: a) NMR solution structure of QK10Nle peptide in H_2O with 10% D_2O at pH 5.5. The ribbon drawing of 20 conformers superimposed a) on the backbone atoms (RMSD values is 0.10 Å) and b) on the heavy atoms (RMSD values is 0.85 Å) of residues from W4 to Y12. c) NMR representative structures of QK10Nle (yellow) and QK (blue) peptides are superimposed (RMSD value for the backbone atoms is 0.68 Å).

Next, structural characterization of the QK10Tle in aqueous solution was performed. NMR analysis of both chemical shifts and NOEs for the QK10Tle peptide pointed out that a helical segment is still characterizing the central region encompassing residues 4–10. Indeed, several NOE contacts characteristic of a helical fold were detected in the segment Trp4-Tle10 (Fig. S6b). A complete structure calculation, conducted with CYANA software, confirmed a helical structuration in the central region of the QK10Tle with both N-terminal and C-terminal largely disordered. The final input file for the CYANA structure calculation software contained 83 meaningful distance constraints (32 intra-residue, 31 short, and 20 medium range) and 72 angle constraints (Table S11). The superimposition of the twenty lowest energy models indicated that the rms deviation values of the backbone and of all heavy atoms of the 4-12 region of QK10Tle are 0.11±0.05 Å and 1.25±0.15 Å, respectively (Figure 6a and b). At last, although QK10Tle appeared mostly disordered, the superposition of the mean structures of QK and QK10Tle clearly pointed out the two peptides.

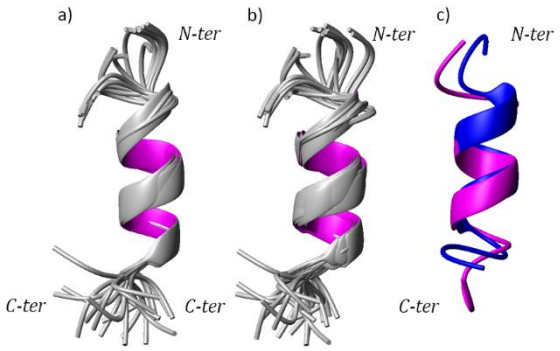

Figure 6: a) NMR solution structure of QK10Tle peptide in H_2O. The ribbon drawing of 20 conformers superimposed a) on the backbone atoms (RMSD values is 0.11 Å) and b) on the heavy atoms (RMSD values is 1.25 Å) of residues from W4 to Y12. c) NMR representative structures of QK10Tle (magenta) and QK (blue) peptides are superimposed (RMSD value for the backbone atoms is 0.72 Å).

To get high resolution structural characterization of QK10Nle helix folding pathway, temperature structural changes have been investigated by NMR spectroscopy. In particular, a series of one-dimensional ^{1}H and bi-dimensional [^{1}H, ^{1}H] TOCSY spectra have been acquired from 298 K to 343 K, at regular intervals of 5 K. At 343 K, QK10Nle Hα chemical shifts are mostly close to their random coil values, indicating a substantial lack of peptide secondary structure (Fig. S8). The analysis of the NMR thermal folding/unfolding curves (Fig. 7) revealed that many of the chemical shifts of single protons could be fitted using a sigmoidal curve, therefore deriving very punctual atomic thermal transitions.[30]

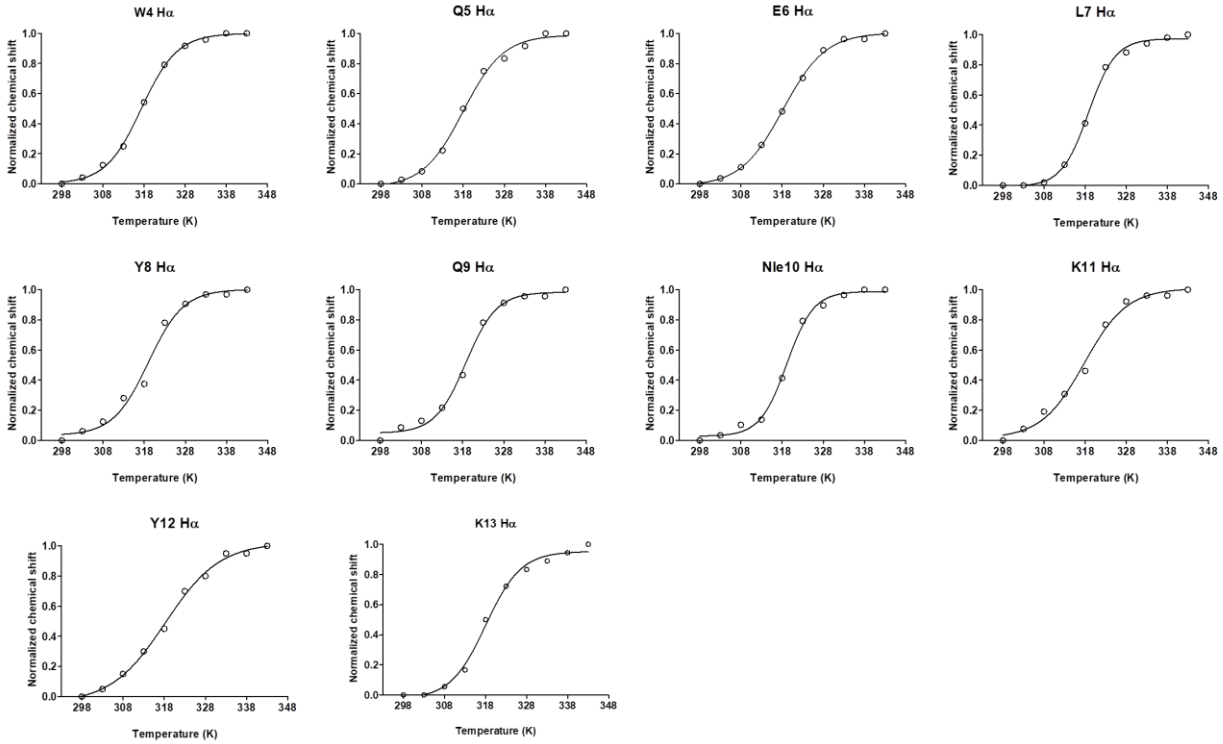

Figure 7: Plot of the Hα chemical shift versus temperature of residues from Trp4 to Lys13 of QK10Nle peptide.

The alpha-protons of the residues in helical organization present very similar T_m included between 317.4 and 319.1 K with a mean value of 318.3 ± 0.5 K; interestingly, protons of the residues Leu7 and Nle10 show significantly higher Tm, respectively of 318.8 and 319.1 K, with a mean value of

319.0 ± 0.3 K. Moreover, Hα chemical shift curves of the remaining residues (Lys1, Leu2, Thr3, Gly14, and Ile15) indicate that they are less sensitive to temperature variations.

4. Discussion

Helix formation and stability have been widely studied using peptide models. Much information on energetics and amino acids role has been derived from folding and design studies. Here we analyze the role of hydrophobic interactions, steric hindrance, chain length on i, i+3 position in QK peptide, a VEGF mimetic helical peptide. We focused our attention on position 10, occupied by a leucine, as previous studies highlighted the role of the Leu7-Leu10 interaction in modulating the helix formation and conferring an unusual thermodynamic stability, which characterizes the thermal unfolding of peptide QK. Following our previous work on QK analogue bearing alanine in position 10 [15], Leu10 has been replaced by hydrophobic amino acids with different side-chain length, hydrophobicity and steric hindrance. Ten peptides were, hence, synthesized and analyzed combining CD, calorimetry and NMR spectroscopy.

The helical content of peptides was measured by CD and NMR and a substantial agreement between the two techniques was found. The peptides showed a different helical content varying from a well-structured helix to partial helical structures. In particular, the replacement of Leu10 results in a very slight increase of helical content for QK10Nle, a slight decrease of helicity for QK10I and QK10Nva and in a significant decrease of helicity for peptides going from QK10Phg to QK10Tle (see Figure 4). The helical propensity of amino acids presenting a linear hydrophobic side-chain, such as Nle, Nva and Abu, was previously studied indicating that these residues are helix-stabilizing with a helical propensity comparable to that of leucine.[36, 37] CD and NMR analysis showed that peptide helical content in QK, instead, depends on the length of the linear side-chain (Nle > Nva > Ala > Abu) as we observed a higher helical content increasing the number of carbon atoms except for Abu. In the context of peptide QK, the different peptide helical content of this set of amino acids is also related to the interaction with the side-chain of Leu7, as already observed for QK10A.[15] We find the result obtained for QK10Abu quite surprising because, even though it was already observed that a helical peptide could be destabilized replacing Ala with Abu,[36] in QK the loss of helical content is remarkable. Furthermore, our data indicate that the presence of a γ-methyl in a linear (Abu) or

branched (Val or Tle) chain is detrimental to peptide helical content and a longer side-chain is required to increase the helical population. In respect to QK helical content, QK10 mutants comprising residues with short side-chains (Tle, Abu, Val, Ala) show a significant lower helical content, those harboring in position 10 amino acids with long side-chains and moderate helical propensities (Ile, Phe) exhibit a moderately reduced helical content, whereas peptides containing amino acids with linear long side-chains and a reported high helical propensity (Nle, Nva) reveal a helical content comparable to QK.

Analyzing the punctual helicity of the peptides (Figure 3), it clearly appears that the first N-terminal turn (residues 4-7) is generally preserved, while the second turn results partially or even entirely lost in the peptides lacking part of QK helical content.

Helical content does not completely correlate with the hydrophobicity of the inserted residues as derived from HPLC retention time of the corresponding peptides, assuming that the difference in peptide hydrophobicity depends only on the specific residue in position 10. This suggests that Leu7-Leu10 hydrophobic interaction is optimized by a specific geometry that could be achieved by large and unconstrained hydrophobic amino acids (Leu, Nleu, Nva). The other QK analogues could not establish an optimal interaction with Leu7 resulting in a drop of the peptide helical content.

The peptide QK is also characterized by an unusual thermal stability that computational and experimental studies have indicated to be based on Leu7-Leu10 hydrophobic interaction.[14] Very interestingly, DSC analysis confirms a strikingly high QK thermal stability with a Tm of 78.3 °C and shows that all QK analogues have much lower thermal stabilities, with Tm comprised between 34.9 and 50.6 °C. More particularly, QK analogues having in position 10 a residue with an aromatic side-chain, such as Phg or Phe, or a short branched side-chain, such as Val or Tle, or a long linear side-chain, such as Nle, possess a very low thermal stability, among 34.9 and 41.2 °C.

We have also determined the NMR high resolution structure of QK10Nleu and QK10Tle peptides, as such QK analogs showed respectively the higher and lower helix populations in the NMR studies. The two structures nicely confirm the secondary structure predictions obtained by the Hα chemical

shifts. QK10Nle is mostly helical, from residue Trp4 to Tyr12, very similarly to what was observed for QK. Nonetheless, comparison of Leu7 – Nle10 side-chains interactions in QK10Nle with those observed between Leu7 and Leu10 in QK indicates that the latter ones are significantly more numerous that the first ones. This experimental evidence further confirms the importance of the hydrophobic interactions between Leu7 and Leu10. QK10Tle retains helical structure only among Trp4 and Tle10 and is less structured, as indicated by the reduced number of NOEs observed. The thermal unfolding mechanism of QK10Nle, as determined by NMR spectroscopy, indicates that the peptide unrolls in a cooperative fashion, with a Tm of 318.3 K, in a good agreement with the DSC data. Such observation could suggest that Leu7-Nle10 interaction is not able to stabilize QK10Nle helix up to 350 K, as Leu7-Leu10 interaction does in QK. We already reported the thermal unfolding of peptide QK10Ala [15] by NMR which is different from that described for QK10Nle, supporting the observation that the change of only one amino acid could induce a different unfolding mechanism. In fact, increasing the temperature, QK10Ala, which is less helical and less thermal stable than QK, presents a stable central turn as transient intermediate structure which acts as nucleation site for the helix formation. QK10Ala peptide cannot make stabilizing interactions with Leu7 in the folded state (helical content drops with respect to QK and QK10Nle) but during the unfolding process can stabilize the central helical turn, probably because of its high helical propensity, resulting in a thermal unfolding process with a melting temperature slightly higher than QK10Nle and a different unfolding mechanism.

A detailed comparison between helical contents and thermal stabilities of QK analogues clearly shows that these two features are uncorrelated in this peptide family. QK peptide results to be highly helical in aqueous solution and possesses, at the same time, a remarkable thermal stability. These two structural properties are at the basis of the very relevant biological VEGF agonistic activity of this peptide. Substituting Leu10, responsible for a decisive hydrophobic side-chain interaction with Leu7, with different hydrophobic residues, the resulting QK analogues may preserve or more often lose a part of their helicity, but they always drastically reduce QK thermal stability. Therefore,

characterizing the thermal unfolding features of structured peptides designed for bio-functional purposes may represent a very useful information to obtain bioactive molecules.

5. Conclusions

Replacing leucine in position 10 of QK peptide with a hydrophobic amino acid both helical content and thermal stability are affected. The variation of peptide helical content and thermal stability are not always correlated, as they independently rely on the type of interaction (strength and geometry) that could be established between Leu7 and the residue in position 10. Overall, leucine in i+3 position showed an advantage over other non-polar amino acids in stabilizing helical peptide by pairwise i, i+3 interaction when a leucine is in position i. Furthermore, analysis of peptide thermal profile appears a useful tool to determine the best residue able to stabilize the conformation of a bioactive helical peptide.

Acknowledgements

We thank Maurizio Amendola and Leopoldo Zona for technical assistance.

Declaration of competing interest

Authors declare no financial interests.

Funding

This research did not receive any specific grant from funding agencies in the public, commercial, or not-for-profit sectors.

References

[1] R. Aurora, T.P. Creamer, R. Srinivasan, G.D. Rose, Local interactions in protein folding: Lessons from the alpha-helix, Journal of Biological Chemistry 272(3) (1997) 1413-1416.
[2] J.M. Scholtz, R.L. Baldwin, The Mechanism of Alpha-Helix Formation by Peptides, Annu Rev Bioph Biom 21 (1992) 95-118.
[3] C.A. Rohl, R.L. Baldwin, Deciphering rules of helix stability in peptides, Energetics of Biological Macromolecules, Pt B 295 (1998) 1-26.
[4] L.D. D'Andrea, G. Iaccarino, R. Fattorusso, D. Sorriento, C. Carannante, D. Capasso, B. Trimarco, C. Pedone, Targeting angiogenesis: Structural characterization and biological properties of a de novo engineered VEGF mimicking peptide, P Natl Acad Sci USA 102(40) (2005) 14215-14220.
[5] L.D. D'Andrea, L. De Rosa, C. Vigliotti, M. Cataldi, VEGF mimic peptides: Potential applications in central nervous system therapeutics, New Horiz Transl Med 3(5) (2017) 233-251.
[6] L. De Rosa, R. Di Stasi, L.D. D'Andrea, Pro-angiogenic peptides in biomedicine, Arch Biochem Biophys 660 (2018) 72-86.
[7] L.D. D'Andrea, A. Romanelli, R. Di Stasi, C. Pedone, Bioinorganic aspects of angiogenesis, Dalton T 39(33) (2010) 7625-7636.
[8] F. Finetti, A. Basile, D. Capasso, S. Di Gaetano, R. Di Stasi, M. Pascale, C.M. Turco, M. Ziche, L. Morbidelli, L.D. D'Andrea, Functional and pharmacological characterization of a VEGF mimetic peptide on reparative angiogenesis, Biochemical Pharmacology 84(3) (2012) 303-311.
[9] G.K. Dudar, L.D. D'Andrea, R. Di Stasi, C. Pedone, J.L. Wallace, A vascular endothelial growth factor mimetic accelerates gastric ulcer healing in an iNOS-dependent manner, Am J Physiol-Gastr L 295(2) (2008) G374-G381.
[10] G. Santulli, M. Ciccarelli, G. Palumbo, A. Campanile, G. Galasso, B. Ziaco, G.G. Altobelli, V. Cimini, F. Piscione, L.D. D'Andrea, C. Pedone, B. Trimarco, G. Iaccarino, In vivo properties of the proangiogenic peptide QK, Journal of Translational Medicine 7 (2009).
[11] G. Pignataro, B. Ziaco, A. Tortiglione, R. Gala, O. Cuomo, A. Vinciguerra, D. Lapi, T. Mastantuono, S. Anzilotti, L.D. D'Andrea, C. Pedone, G. di Renzo, L. Annunziato, M. Cataldi, Neuroprotective Effect of VEGF-Mimetic Peptide QK in Experimental Brain Ischemia Induced in Rat by Middle Cerebral Artery Occlusion, Acs Chem Neurosci 6(9) (2015) 1517-1525.
[12] A. Verheyen, E. Peeraer, D. Lambrechts, K. Poesen, P. Carmeliet, M. Shibuya, I. Pintelon, J.P. Timmermans, R. Nuydens, T. Meert, Therapeutic Potential of Vegf and Vegf-Derived Peptide in Peripheral Neuropathies, Neuroscience 244 (2013) 77-89.
[13] B. Ziaco, D. Diana, D. Capasso, R. Palumbo, V. Celentano, R. Di Stasi, R. Fattorusso, L.D. D'Andrea, C-terminal truncation of Vascular Endothelial Growth Factor mimetic helical peptide preserves structural and receptor binding properties, Biochem Bioph Res Co 424(2) (2012) 290-294.
[14] D. Diana, B. Ziaco, G. Colombo, G. Scarabelli, A. Romanelli, C. Fedone, R. Fattorusso, L.D. D'Andrea, Structural determinants of the unusual helix stability of a De Novo engineered vascular endothelial growth factor (VEGF) mimicking peptide, Chem-Eur J 14(14) (2008) 4164-4166.
[15] D. Diana, B. Ziaco, G. Scarabelli, C. Pedone, G. Colombo, L.D. D'Andrea, R. Fattorusso, Structural Analysis of a Helical Peptide Unfolding Pathway, Chem-Eur J 16(18) (2010) 5400-5407.
[16] T.L. Hwang, A.J. Shaka, Water Suppression That Works - Excitation Sculpting Using Arbitrary Wave-Forms and Pulsed-Field Gradients, J Magn Reson Ser A 112(2) (1995) 275-279.
[17] C. Dalvit, Efficient multiple-solvent suppression for the study of the interactions of organic solvents with biomolecules, J Biomol Nmr 11(4) (1998) 437-444.
[18] M. Rance, O.W. Sorensen, G. Bodenhausen, G. Wagner, R.R. Ernst, K. Wuthrich, Improved spectral resolution in cosy 1H NMR spectra of proteins via double quantum filtering, Biochem Biophys Res Commun 117(2) (1983) 479-85.
[19] T.D. Goddard, D.G. Kneller, SPARKY 3, University of San Francisco: California,2004.
[20] R.L.J. Keller, The Computer Aided Resonance Assignement Tutorial, CANTINA Verlag2004.

[21] P. Guntert, Automated NMR structure calculation with CYANA, Methods Mol Biol 278 (2004) 353-78.
[22] R. Koradi, M. Billeter, K. Wuthrich, MOLMOL: a program for display and analysis of macromolecular structures, J Mol Graph 14(1) (1996) 51-5, 29-32.
[23] L. Shröndinger The PyMOL molecular graphics system, The PyMOL molecular graphics system, 2010.
[24] M.L. Martin, J.J. Delpuech, G.J. Martinand, Practical NMR spectroscopy, Heyden, London1980.
[25] D. Markovic, S. Proll, C. Bubenzer, H. Scheer, Myoglobin with chlorophyllous chromophores: influence on protein stability, Biochim Biophys Acta 1767(7) (2007) 897-904.
[26] A. Partida-Hanon, M.A. Trevino, M. Mompean, M.A. Jimenez, M. Bruix, Structural insight into the XTACC3/XMAP215 interaction from CD and NMR studies on model peptides, Biopolymers 107(11) (2017).
[27] K. Wüthrich, NMR of Proteins and Nucleic Acids, 1989.
[28] M. Pappalardo, D. Milardi, D. Grasso, C. La Rosa, Phase behaviour of polymer-grafted DPPC membranes for drug delivery systems design, J Therm Anal Calorim 80(2) (2005) 413-418.
[29] R. Guzzi, C. LaRosa, D. Grasso, D. Milardi, L. Sportelli, Experimental model for the thermal denaturation of azurin: A kinetic study, Biophys Chem 60(1-2) (1996) 29-38.
[30] M. Palmieri, G. Malgieri, L. Russo, I. Baglivo, S. Esposito, F. Netti, A. Del Gatto, I. de Paola, L. Zaccaro, P.V. Pedone, C. Isernia, D. Milardi, R. Fattorusso, Structural Zn(II) Implies a Switch from Fully Cooperative to Partly Downhill Folding in Highly Homologous Proteins, J Am Chem Soc 135(13) (2013) 5220-5228.
[31] G. Arena, R. Fattorusso, G. Grasso, G.I. Grasso, C. Isernia, G. Malgieri, D. Milardi, E. Rizzarelli, Zinc(II) Complexes of Ubiquitin: Speciation, Affinity and Binding Features, Chem-Eur J 17(41) (2011) 11596-11603.
[32] N.J. Greenfield, Using circular dichroism spectra to estimate protein secondary structure, Nat Protoc 1(6) (2006) 2876-2890.
[33] A. Chakrabartty, T. Kortemme, S. Padmanabhan, R.L. Baldwin, Aromatic Side-Chain Contribution to Far-Ultraviolet Circular-Dichroism of Helical Peptides and Its Effect on Measurement of Helix Propensities, Biochemistry 32(21) (1993) 5560-5565.
[34] D.S. Wishart, B.D. Sykes, Chemical shifts as a tool for structure determination, Methods Enzymol 239 (1994) 363-92.
[35] D.S. Wishart, B.D. Sykes, F.M. Richards, The Chemical-Shift Index - a Fast and Simple Method for the Assignment of Protein Secondary Structure through Nmr-Spectroscopy, Biochemistry 31(6) (1992) 1647-1651.
[36] S. Padmanabhan, R.L. Baldwin, Straight-Chain Nonpolar Amino-Acids Are Good Helix-Formers in Water, Journal of Molecular Biology 219(2) (1991) 135-137.
[37] P.C. Lyu, J.C. Sherman, A. Chen, N.R. Kallenbach, Alpha-Helix Stabilization by Natural and Unnatural Amino-Acids with Alkyl Side-Chains, P Natl Acad Sci USA 88(12) (1991) 5317-5320.